Interfaces between CdTe and ALD Al_2O_3

Craig L. Perkins[1], Tursun Ablekim[1], Teresa M. Barnes[1], Darius Kuciauskas[1], Kelvin G. Lynn[2], William Nemeth[1], Matthew O. Reese[1], Santosh K. Swain[2], and Wyatt K. Metzger[1]

[1]National Renewable Energy Laboratory, Golden CO 80401 USA

[2]Center for Materials Research, Washington State University, Pullman, WA 99164-2711, USA

Abstract — **We present a combination of X-ray photoelectron spectroscopy (XPS) and time-resolved photoluminescence (TRPL) to probe the details of interface formation between CdTe and alumina deposited by atomic layer deposition (ALD). Alumina ALD using water as the oxygen source causes the elimination of Te oxides that are initially present on air-exposed CdTe surfaces. TRPL on the resulting CdTe interface indicates some degree of passivation. On the other hand, post growth treatment of Al_2O_3/CdTe structures with $CdCl_2$ and oxygen causes regrowth of Te oxides. Some of these structures show improved lifetimes, thereby pointing towards a critical role for Te oxides in interfacial CdTe passivation by Al_2O_3. Direct measurement of band positions with XPS indicates that the passivation is caused primarily by chemical rather than field effect mechanisms.**

I. Introduction

A recent surge in the interest of interfaces between CdTe and aluminum oxides has been driven by several factors. It has been known for some time that when using water as the source of oxygen, alumina ALD on silicon surfaces causes the release of atomic hydrogen that helps passivate dangling bonds in the silicon near surface.[1] In addition to this chemical passivation, alumina can bring about field-effect passivation in both n and p-type silicon because of its ability to trap negative fixed charge. The combination of these effects has resulted in low recombination velocities and high efficiencies in silicon-based photovoltaic devices. Furthermore, alumina passivation in polycrystalline CdTe and CdSeTe double heterostructures has yielded unprecedented lifetimes exceeding 100 ns.[2] As alumina is not an appropriate contact in standard photovoltaic devices, in this work we seek to understand the fundamental mechanisms driving this passivation to develop similar passivation approaches that will significantly enhance aggregate lifetime and performance in CdTe photovoltaics.

Alumina has also seen use in thin film photovoltaics with materials such as $Cu(In,Ga)Se_2$ and CdTe. Liang et al. used nm-scale ALD alumina layers to improve CdTe back contacts.[3] Patterned sputter-grown alumina has been found to passivate both the front and back of CdTe devices.[2] Bissig and coworkers found that using alumina to passivate cross sections of CdTe solar cells during electron beam-induced current (EBIC) experiments allowed them to gain a better understanding of current collection in their devices.[4] In these works, the tentative explanations for the passivation effect mirror what is known from the silicon literature: negative fixed charge at the interface of a p-type material should cause upward band bending and induce field effect passivation. However, the anticipated changes that should accompany upward band bending, a decrease in the core level binding energies, was not observed in the XPS data of Ref [3]. Further motivating our current work is the fact that previous work on alumina passivated back contacts may have inadvertently probed CuTe-alumina interfaces rather than CdTe-alumina interfaces.[2], [5] The copper used in common back contacting schemes is known to produce CuTe phases that segregate to the surface.[6], [7] Currently, little is known about the evolution of the chemical and electronic properties of CdTe as its interface forms with alumina during ALD.

II. Experimental Methods

Phosphorus-doped single crystal CdTe was grown as described in Ref. [8] Single crystal wafers were cut from boules, mechanically polished, etched in Br_2/methanol, then annealed briefly at 250 °C in an inert atmosphere.

Alumina was grown by atomic layer deposition using trimethylaluminum (TMA) and water at a substrate temperature of 200 °C. A control sample ("bare" or "uncoated") was subjected to the same deposition temperature and reactor ambient but no ALD cycles. XPS and TRPL measurements were conducted on the same set of crystals at different stages of the various processing steps. Vapor phase $CdCl_2$ treatment was performed as described previously.[9]

One photon TRPL was carried out as described previously.[10] XPS was performed using a PHI 5600 system described previously.[11] The spectrometer binding energy scale was calibrated using sputter-cleaned metal foils at low and high kinetic energy. CdTe crystals were mounted on graphite foil or carbon tape to help avoid electric potential shifts during XPS measurements. X-ray power dependent measurements were done on core level peaks to ensure that the Fermi energy of the spectrometer and that of the area being probed are not significantly different. Samples generally were measured first at high (350 W) and low (10 W) anode power. When necessary, valence band positions taken at full power, 350 W, were corrected for peak shifts relative to lower power operation.

Pursuant to the DOE Public Access Plan, this document represents the authors' peer-reviewed, accepted manuscript. The published version of the article is available from the relevant publisher.

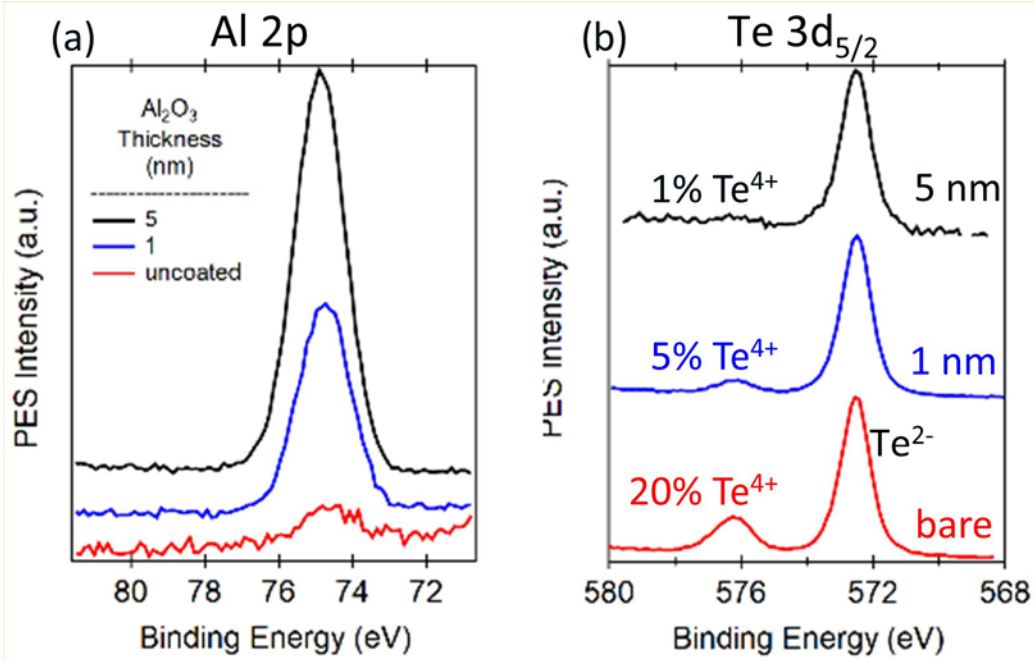

Figure 1. XPS spectra of Al 2p and Te $3d_{5/2}$ regions for crystals with different thicknesses of ALD alumina

III. Results and Discussion

Fig.1 shows high-resolution core level spectra for aluminum and tellurium during different stages of alumina deposition. As expected, the intensity of the Al 2p core level rises with increasing thickness of alumina (Fig. 1a). In our case, 1 nm of alumina corresponds to eight ALD cycles and 5 nm to 42 ALD cycles. A small amount of aluminum was found to be deposited on the control sample that experienced the standard reaction conditions but no ALD cycles (bottom red trace, "uncoated", Fig. 1a). Fig. 1b shows Te $3d_{5/2}$ spectra for the same three samples. These spectra generally show two chemical components: a peak at 572.4 eV corresponding to Te^{2-} and a peak at 576.3 eV corresponding to oxidized tellurium, Te^{4+}. The data in Fig. 1b are normalized in intensity to the Te^{2-} component to allow comparison of the relative contribution of oxidized tellurium. For alumina thicknesses greater than about 5 nm, it was not possible to obtain spectra from the CdTe substrate, which is consistent with the expected XPS probe depth (0-6 nm). Spectra from the uncoated sample display a fairly large percentage of Te^{4+} from the CdTe native oxide. Interestingly, as the number of ALD cycles increases, the relative percentage of oxidized tellurium decreases and then completely disappears after the 42 cycles used to deposit 5 nm of alumina. It should be noted that the probe depths *into the CdTe* for samples with different alumina thickness are somewhat different because of the overlying alumina: data from the sample with 5 nm of alumina probes only a very short distance (<1 nm) into the CdTe, whereas data from the uncoated sample originates from as deep as 6 nm. This means that the reduction of the Te oxides is more dramatic than what seems apparent in Fig. 1b. We attribute the CdTe native oxide reduction to a reaction

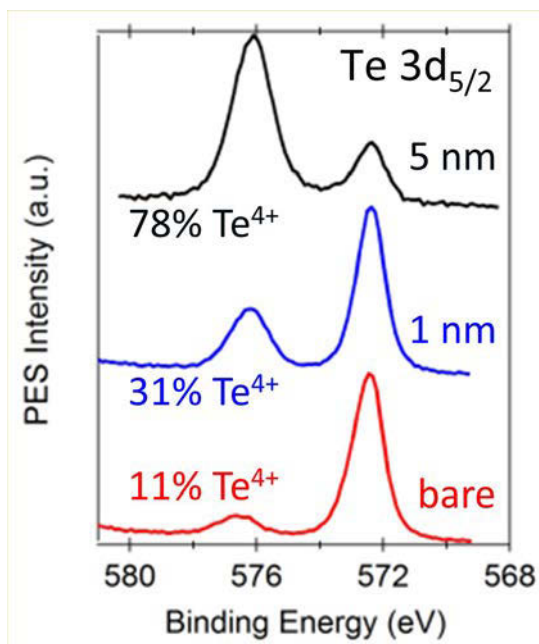

Figure 2. XPS spectra of CdTe crystals with different alumina thicknesses and showing the two chemical states of tellurium found after $CdCl_2/O_2$ treatment.

Pursuant to the DOE Public Access Plan, this document represents the authors' peer-reviewed, accepted manuscript. The published version of the article is available from the relevant publisher.

involving either atomic hydrogen released during the ALD reaction OR from direct reduction by trimethylaluminum. Previous workers have shown that hydrogen released in the TMA + water reaction originates from water rather than from the methyl groups of TMA.[12] Further understanding of the mechanism by which Te^{4+} is reduced in this reaction could come about by replacing water with oxygen or ozone as the oxygen source. If reduction were still observed, then it is likely that TMA itself is the reducing agent as has been observed for copper in CuO surfaces.[13] In this case reduction of Cu^{2+} to Cu^{1+} occurs during ALD with TMA and molecular oxygen, and as a result of a direct interaction between copper and TMA.

In a previous successful use of alumina to passivate CdTe interfaces, the device and thus the interface itself was subjected to $CdCl_2$ treatment.[2] For that reason, we tested the idea that the CdTe-alumina interface evolves further during post-growth $CdCl_2$ treatment. Fig. 2 shows the effects of $CdCl_2/O_2$ treatment on tellurium oxidation.

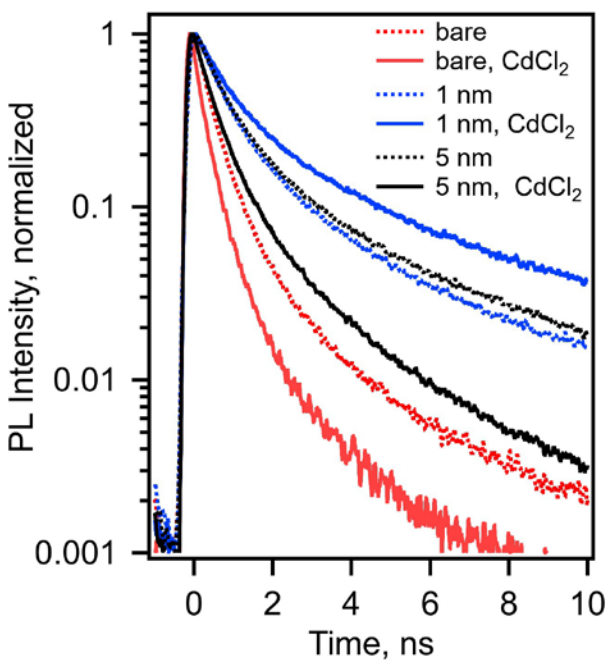

Figure 3. TRPL of alumina/CdTe crystals before and after $CdCl_2/O_2$ treatment.

Clearly, $CdCl_2$ treatment causes oxidation of the CdTe underlying the ALD alumina layers, a process that is especially apparent in the crystal with 5 nm of alumina. This is perhaps related again to the depth probed into the CdTe: data from the sample without alumina ("bare") includes more signal from the unoxidized bulk than do the spectra of the two alumina-coated samples.

Surface passivation of these samples was measured by TRPL. Figure 3 shows TRPL data from alumina-coated crystals before and after $CdCl_2$ treatment. Lifetimes in samples with "as deposited" alumina generally increased, albeit with insignificant changes when the alumina thickness is increased beyond 1 nm. After $CdCl_2/O_2$ treatment, lifetime in the sample 5 nm of alumina decreased. In contrast, $CdCl_2$ treatment increased lifetime to ~16 ns in the sample with 1 nm of alumina.

To directly test whether the changes in lifetimes were the result of field effects, XPS was used to measure the position of the Fermi energy in the CdTe near the alumina interface. By measuring the core-level to valence band separation on clean, well-ordered single crystal CdTe, it was possible to use the Te $3d_{5/2}$ and Cd $3d_{5/2}$ peak positions to monitor the evolution of the CdTe valence band at the buried interface. From earlier work we assume that the bulk doping was not changed by $CdCl_2$ processing.[14] Thus the XPS-measured valence band edge is a measure of the band bending and electric field at the CdTe-alumina interface. Fig. 4 shows Fermi level-referenced valence band maxima for samples with varying thicknesses of alumina before and after $CdCl_2$ treatment. Note that this figure is drawn in the convention of band diagrams such that E_F-E_{VBM} = 0 at the top of the graph corresponds to degenerate p-type surface and E_F-E_{VBM}=1.5 eV corresponds to a degenerate n-type surface.

Figure 4 shows that the bare CdTe crystal is only slightly p-type with the Fermi energy slightly above mid-gap (E_F-E_{VBM} = 0.60 eV). Depositing 1 nm of alumina on this surface causes

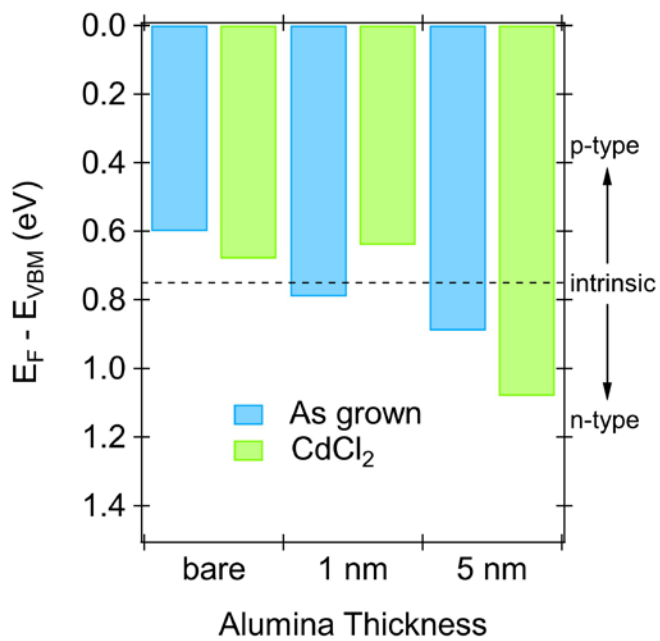

Figure 4. Fermi energy-referenced valence band maxima for uncoated and alumina-coated CdTe crystals before and after $CdCl_2$ treatment.

downward band bending, dropping the valence band to 0.79 eV below the Fermi energy and making the interface slightly

Pursuant to the DOE Public Access Plan, this document represents the authors' peer-reviewed, accepted manuscript. The published version of the article is available from the relevant publisher.

n-type. Increasing the thickness of alumina to 5 nm further increases the downward band bending, with the VBM located 0.89 eV below E_F. Despite this increased electric field in the CdTe in samples with 1 and 5 nm of as-grown alumina, the TRPL data in Figure 3 shows that carrier lifetimes were increased. Thus, we attribute the increased lifetime in these samples to chemical rather than field effect passivation. We note that in our previous work, hydrogen was shown to yield moderate improvement in the surface recombination velocity on CdTe surfaces, and it seems plausible that in the case of as-deposited alumina, some chemical passivation occurred due to the release of hydrogen during the ALD process.[15]

Figure 4 also indicates that $CdCl_2$ treatment of the alumina-coated crystals causes disparate changes in interface passivation. The uncoated and sample with 5 nm of alumina show increased downward band bending after $CdCl_2$, which explains in part the worsened lifetimes seen in Figure 3. In contrast, $CdCl_2$ treatment causes a reduction in downward band bending in the sample with 1 nm of alumina. None of the observed valence band positions are consistent with significant *net* fixed negative charge from the alumina layer, which should cause upward band bending and decrease the observed E_F-E_{VBM} values. We note that as with other alumina interfaces, it is the competition between positive charges directly at the interface and negative charges within the bulk of the alumina that determine the net charge and changes in band bending in alumina's interfacial partner.[16] Thus, it is possible that alternative interface engineering or simply thicker alumina could bring out both field effect and chemical passivation in the CdTe and alumina material set. Finally, we note that the CdTe interface showing best passivation by TRPL (1 nm of alumina, $CdCl_2$-treated), has undergone several major chemical changes (hydrogenation, oxidation, chlorination) but has a surface electric field similar to the starting surface. For that reason, it appears that chemical passivation, one characterized by the formation of a CdTe oxide and the presence of chlorine, can be the dominant mechanism for improving TRPL lifetime in the alumina/CdTe system.

IV. CONCLUSIONS

A schematic of the evolution of the CdTe/alumina interface during atomic layer deposition and post-growth $CdCl_2$ treatment is shown in Fig. 5. The ALD reaction between trimethylaluminum and water causes reduction of the CdTe native oxide initially present and the eventual formation of an abrupt CdTe/alumina interface. TRPL indicates some passivation occurs with as-deposited alumina. XPS-based band bending measurements indicated that this passivation is not from a decreased surface electric field. Post-growth treatment of the alumina/CdTe crystals with $CdCl_2/O_2$ causes a thin layer of CdTe oxide to form between the alumina and CdTe layers. Ongoing and previous work[17] indicates that chlorine is present in an atomically thin layer of $CdCl_2$ between the alumina and CdTe as depicted in Fig. 5. For an alumina thickness of 1 nm, TRPL lifetimes increase substantially upon this post-growth oxidation and chlorination. Direct measurements of the CdTe band positions at the alumina interface are generally indicative of downward band bending, inconsistent with net fixed negative charge at this CdTe/alumina interface. The sum of these measurements indicates that passivation of CdTe surfaces by alumina can occur by chemical means, and implicates CdTe oxides as being important to the passivation mechanism.

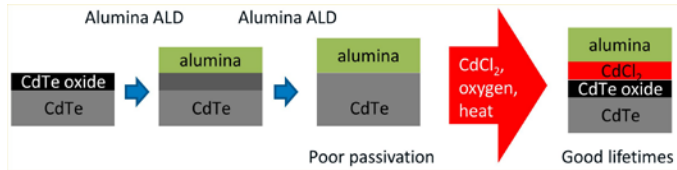

Figure 5. Schematic of the evolution of the ALD alumina/CdTe interface showing reduction and loss of the initially present CdTe native oxide and reformation of the oxide layer during $CdCl_2/O_2$ processing.

IV. ACKNOWLEDGMENTS

This work was authored by Alliance for Sustainable Energy, LLC, the manager and operator of the National Renewable Energy Laboratory for the U.S. Department of Energy (DOE) under Contract No. DE-AC36-08GO28308. Funding provided by U.S. Department of Energy Office of Energy Efficiency and Renewable Energy Solar Energy Technologies Office under agreement 30307. The views expressed in the article do not necessarily represent the views of the DOE or the U.S. Government. The U.S. Government retains and the publisher, by accepting the article for publication, acknowledges that the U.S. Government retains a nonexclusive, paid-up, irrevocable, worldwide license to publish or reproduce the published form of this work, or allow others to do so, for U.S. Government purposes.

REFERENCES

[1] G. Dingemans and W. M. M. Kessels, "Status and prospects of Al2O3-based surface passivation schemes for silicon solar cells," *J. Vac. Sci. Technol. Vac. Surf. Films*, vol. 30, no. 4, p. 040802, Jul. 2012.

[2] J. M. Kephart *et al.*, "Sputter-Deposited Oxides for Interface Passivation of CdTe Photovoltaics," *IEEE J. Photovolt.*, vol. PP, no. 99, pp. 1–7, 2018.

[3] J. Liang *et al.*, "Rectification and tunneling effects enabled by Al_2O_3 atomic layer deposited on back contact of CdTe solar cells," *Appl. Phys. Lett.*, vol. 107, no. 1, p. 013907, Jul. 2015.

[4] B. Bissig *et al.*, "On a better estimate of the charge collection function in CdTe solar cells: Al2O3 enhanced electron beam induced current measurements," *Thin Solid Films*, vol. 633, pp. 218–221, Jul. 2017.

Pursuant to the DOE Public Access Plan, this document represents the authors' peer-reviewed, accepted manuscript. The published version of the article is available from the relevant publisher.

[5] Q. Lin *et al.*, “A novel p-type and metallic dual-functional Cu–Al2O3 ultra-thin layer as the back electrode enabling high performance of thin film solar cells,” *Chem. Commun.*, vol. 52, no. 71, pp. 10708–10711, Aug. 2016.
[6] G. Teeter, “The reaction kinetics of Cu with the CdTe(111)-B surface: Formation of metastable CuxTe(x∼2),” *J. Chem. Phys.*, vol. 123, no. 18, p. 184713, Nov. 2005.
[7] G. Teeter, “X-ray and ultraviolet photoelectron spectroscopy measurements of Cu-doped CdTe(111)-B: Observation of temperature-reversible CuxTe precipitation and effect on ionization potential,” *J. Appl. Phys.*, vol. 102, no. 3, p. 034504, Aug. 2007.
[8] T. Ablekim, S. K. Swain, D. Kuciauskas, N. S. Parmar, and K. G. Lynn, “Fabrication of single-crystal solar cells from phosphorous-doped CdTe wafer,” in *2015 IEEE 42nd Photovoltaic Specialist Conference (PVSC)*, 2015, pp. 1–4.
[9] D. M. Meysing *et al.*, “Evolution of oxygenated cadmium sulfide (CdS:O) during high-temperature CdTe solar cell fabrication,” *Sol. Energy Mater. Sol. Cells*, vol. 157, pp. 276–285, Dec. 2016.
[10] D. Kuciauskas *et al.*, “Minority Carrier Lifetime Analysis in the Bulk of Thin-Film Absorbers Using Subbandgap (Two-Photon) Excitation,” *IEEE J. Photovolt.*, vol. 3, no. 4, pp. 1319–1324, Oct. 2013.
[11] C. L. Perkins and F. S. Hasoon, “Surfactant-assisted growth of CdS thin films for photovoltaic applications,” *J. Vac. Sci. Technol. Vac. Surf. Films*, vol. 24, no. 3, pp. 497–504, 2006.
[12] C. Guerra-Nuñez, M. Döbeli, J. Michler, and I. Utke, “Reaction and Growth Mechanisms in Al2O3 deposited via Atomic Layer Deposition: Elucidating the Hydrogen Source,” *Chem. Mater.*, vol. 29, no. 20, pp. 8690–8703, Oct. 2017.
[13] A. Gharachorlou *et al.*, “Trimethylaluminum and Oxygen Atomic Layer Deposition on Hydroxyl-Free Cu(111),” *ACS Appl. Mater. Interfaces*, vol. 7, no. 30, pp. 16428–16439, Aug. 2015.
[14] “Joel Duenow, personal communication.” .
[15] M. O. Reese *et al.*, “Intrinsic surface passivation of CdTe,” *J. Appl. Phys.*, vol. 118, no. 15, p. 155305, Oct. 2015.
[16] D. K. Simon, P. M. Jordan, T. Mikolajick, and I. Dirnstorfer, “On the Control of the Fixed Charge Densities in Al2O3-Based Silicon Surface Passivation Schemes,” *ACS Appl. Mater. Interfaces*, vol. 7, no. 51, pp. 28215–28222, Dec. 2015.
[17] C. L. Perkins, C. Beall, M. O. Reese, and T. M. Barnes, “Two-Dimensional Cadmium Chloride Nanosheets in Cadmium Telluride Solar Cells,” *ACS Appl. Mater. Interfaces*, vol. 9, no. 24, pp. 20561–20565, Jun. 2017.

Pursuant to the DOE Public Access Plan, this document represents the authors' peer-reviewed, accepted manuscript. The published version of the article is available from the relevant publisher.